Proceedings of the 32nd European Safety and Reliability Conference (ESREL 2022)
Edited by Maria Chiara Leva, Edoardo Patelli, Luca Podofillini, and Simon Wilson

Published by Research Publishing, Singapore.
doi: 10.3850/978-981-18-5183-4_S04-06-621-cd

Prediction of the Remaining Useful Life of MOSFETs Used in Automotive Inverters by an Ensemble of Neural Networks

Giovanni Floreale

Energy Department, Politecnico di Milano, Milan, Italy. giovanni.floreale@polimi.it

Piero Baraldi

Energy Department, Politecnico di Milano, Milan, Italy. E-mail: piero.baraldi@polimi.it

Enrico Zio

MINES Paris-PSL, CRC, Sophia Antipolis, Energy Department, Politecnico di Milano, Milan, Italy
E-mail: enrico.zio@polimi.it

Carlo Cecati

University of L'Aquila -DISIM and DigiPower Ltd. L'Aquila, Italy. carlo.cecati@univaq.it

Concettina Buccella

University of L'Aquila -DISIM and DigiPower Ltd. L'Aquila, Italy. concettina.buccella@univaq.it

Stefano Galeazzi

2T srl, Poggiofiorito (CH) - Italy. E-mail: stefano.galeazzi@duet.it

Francesco Barcio

TEKNE srl, Poggiofiorito (CH) - Italy. f.barcio@tekne.it

Carlo Tieri

TEKNE srl, Poggiofiorito (CH) – Italy. c.tieri@tekne.it

Failures of the switches of Electric Vehicles (EV) inverters can cause the unavailability of the vehicles powertrain. For this, the automotive industry is interested in methods for the prediction of the Remaining Useful Life (RUL) of switches, such as MOSFETs. In this regard, the main challenges are: *a*) due to the variations of the measured signals MOSFETs' degradation can be hidden by the inherent signals variability due to the continuously changing operating conditions in automotive applications; *b*) the scarcity of data collected from in-field applications.

In the present work, we develop a Simulink model for simulating the evolution of physical quantities correlated to MOSFETs' degradation, such as temperatures and electrical signals, during run-to-failure degradation trajectories. Then, a prognostic model based on the use of an ensemble of Artificial Neural Networks which receive in input sliding windows of the measured signals, is developed for predicting the MOSFETs' RUL. The model is validated considering a H-bridge inverter made of four MOSFETs.

Keywords: Remaining Useful Life, Prognostics, Electric Vehicles, Inverter, Artificial Neural Network.

1. Introduction

Inverters are among the most critical systems of the powertrain of EV since their failure can cause the vehicle loss of control (Ni, et al. 2020).

In this work, we consider switches, which being subject to high-frequency thermal swings that cause severe thermomechanical stresses, are the principal cause of failure of inverters

(Banerjee, Putcha and Gupta 2021). Therefore, predicting the RUL of switches, i.e. the time interval between the present and failure (Singh and Pahuja 2018), can be beneficial with respect to the reduction of unscheduled maintenance interventions and the optimization of the inverter lifecycle. Generally, prognostic methods for the prediction of components' RUL are classified as physics-based, data-driven and hybrid (Si, et al. 2011) (Niu 2017) (Sutharssan, et al. 2015). A limitation of physics-based methods for the prediction of the RUL of inverters' switches is the difficulty of accurately describing the impact of the large range of Operating and Environmental Conditions (OEC), which are typically experienced in automotive applications, on the degradation process (Ji, et al. 2013). On the other side, the development of data-driven prognostic methods is challenged by the lack of failure data. Although Accelerated Aging Tests (AATs) can be in principle performed in laboratories to investigate the degradation of power electronic devices and collect real data, their effective implementation is limited by their cost and the difficulty of reproducing the large range of OEC experienced in real applications (Ji, et al. 2013). In this context, the present work develops a physics-based simulator of a H-bridge inverter with four MOSFETs used as switches (Dusmez, Duran and Akin 2016) to collect the data needed for the training of a data-driven prognostic method. It allows simulating several run-to-failure trajectories considering the uncertainties affecting the OEC, the sensor measurements, the device characteristics and the degradation process itself. The simulated data are, then, used to train a data-driven prognostic method based on an ensemble of ANNs, which receive in input sliding windows of the signals measurements. The ensemble on ANNs is obtained by randomly splitting the training set into subsets, and using a different combination of subsets to train each ANN. The predictions of the ANNs of the ensemble are aggregated by computing their median value, which has been shown to be more robust than other statistical indicators (Kourentzes, Barrow and Crone 2014). The use of sliding windows of the signal values as input of the ANNs allows capturing the dynamic behaviour of the system, considering the correlation of signals in different timesteps.

The rest of the work is organized as follows: in Section 2, the considered H-bridge configuration is described; in Section 3, the simulator of the MOSFET and the associated degradation model are discussed; Section 4 describes the developed prognostic methodology; Section 5 discusses the obtained results and finally, Section 6 provides the work conclusions and future developments.

2. H-bridge Inverter

The H-bridge is a very common converter topology, and can be found in many different conversion systems, including, in automotive, inverter and battery management systems. A H-bridge contains two legs, each one with two switching elements and with their antiparallel diodes, the load at the center (Figure 1). Adding a third leg in parallel to the other two leads to a three phase inverter. Therefore, the H-bridge is representative of the majority of power converter topologies. The switches can be power MOSFETs or IGBTs; in this work we consider MOSFETs, which are preferred in medium power applications with voltage ratings up to 300Vdc and for operations at high frequencies (tenth-hundreds kHz). IGBTs have at higher voltage rating (typically 1200V) but lower switching frequency, and are preferred in three phase systems operating at 600Vdc.

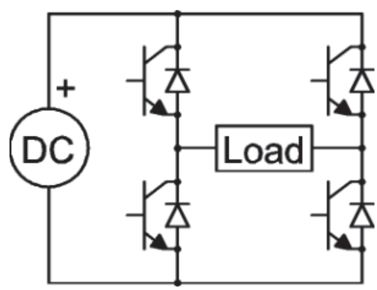

Figure 1: scheme of the H-bridge inverter.

2.1 Degradation Mechanisms

MOSFETs turn on/off at high frequencies to produce the desired output patterns and control the electrical load, e.g. the motor speed (Khan, Khan and Saleque 2018). When the MOSFET is in conduction state, current flows through it, heats it up, whereas when the MOSFET is open and the current cannot flow, the temperature decays. Losses depend on the conduction state through the drain source on-resistance (Rds) and on the number of switches per second (switching losses). The layers of MOSFETs, which are typically characterized by different thermal properties, have great influence on the heating and cooling rates of the device and determine its overall performance. Moreover, due to the high switching rate, dynamic and differential solicitations of their layers are significant. Consequently, the failures of power devices are directly related to the their physical structure and packaging technology (Ciappa 2002). During thermal and/or thermo-mechanical loadings, the bimetallic effect causes that the layers experience shear stresses due to their differing coefficients of thermal expansion (CTE). Then, fatigues, cracks, delamination, or complete lift-offs can occur with the consequence of increasing Rds (Dusmez, Duran and Akin 2016). The weak points are the interconnections inside the power device which include wire bonds and solder joints between die and output pins. The most common failures occur at the interconnections of adjacent materials: wire bond and silicon, silicon and Direct Bonded Copper (DBC) substrate, DBC substrate and base plate (Kovačević, Drofenik and Kolar 2010).

MOSFETs failures can be caused by overstress or wear-out. The former is a sudden event generally caused by overcurrent/overvoltage difficult to predict and that can be avoided if the H-bridge has been correctly designed and realized and the switches work in their operational ranges, whereas the latter is a long-term process which, in principle, can be anticipated. For this reason, this work will focus on the prediction of wear-out.

3. Simulation of the degradation data

Due to the lack of real data, we develop a simulator to collect the run-to-failure trajectories needed for the development of the prognostic model. It combines a model, $M_{H-bridge}$, of the H-bridge behavior with a model, M_{deg}, of the switch degradation. The model $M_{H-bridge}$ receives in input the electrical resistance of the H-bridge switches (Rds) and provides in output the evolution of the electrical and environment signals, $\bar{\bar{x}}$, such as currents, voltages and temperatures, during operation. The obtained switch junction temperature, T_j, which determines the stress level, becomes, then, an input of the degradation model (M_{deg}), which provides in output the component degradation, *D*. Finally, the electrical resistance of the switches (Rds) is obtained from the component degradation, *D*, through a third model M_{res}. The loop is repeated, updating the degradation every Δi thermal cycles, until a failure occurs, i.e. the degradation *D* reaches 1, according to the scheme of Figure 2.

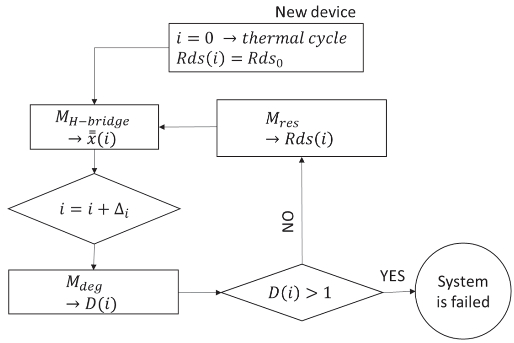

Figure 2: simulation of a run to failure trajectory, Rds_0 is the nominal value of the switch drain source resistance.

Subsections 3.1, 3.2 and 3.3 will describe the model of the H-bridge, $M_{H-bridge}$, the degradation model, M_{deg}, and the model for linking the degradation to the electrical resistance of the switches, M_{res}, respectively. The description will be made considering AATs, which consist of the repetition of power cycles to accelerate the component degradation through the induction of thermal swing effects, performed under fixed operational conditions. Specifically, the thermal cycle of the simulated AAT starts at ambient temperature (298K) and is stopped when the case temperature (T_{case}) reaches 400K. The choice of simulating run-to-failure trajectories during AATs is motivated by the fact that it is expected that AATs will be performed in laboratories within the European project "iRel40 Intelligent Reliability 4.0", to validate the developed simulator.

3.1. H-bridge model

The H-bridge model ($M_{H-bridge}$) is used to simulate the signal behaviors in new and degraded devices. For each thermal cycle of duration T^c, it receives in input Rds and a vector $\vec{o}$ containing the OEC and it provides in output the time evolution of 9 physical quantities represented by the matrix $\bar{\bar{x}}$ of size [9, T^c], whose general element $x_i(j)$ is the value of the $i-th$ variable at time j. Table 1 reports input and output quantities of the $M_{H-bridge}$ model.

To properly represent the stochasticity affecting the behaviour of the real inverters, the following sources of uncertainty are considered in the simulations:

Table 1: list of the input and output quantities of the $M_{H-bridge}$ model.

INPUT			OUTPUT		
Physical Degradation indicator	R_{DS}	Drain Source resistance	Time evolution of the physical quantities during a thermal cycle: $\bar{\bar{x}}$	$\vec{x_1}(1{:}T^c)= T_j$	Junction Temperature
Operational conditions $\vec{o}$	$o_1 = T_{ext}$	External Temperature		$\vec{x_2}(1{:}T^c)= T_{case}$	Case temperature
				$\vec{x_3}(1{:}T^c)= T_{diss}$	Dissipator Temperature
	$o_2 = R_{load}$	Load resistance		$\vec{x_4}(1{:}T^c)= V_{GS}$	Gate-Source Voltage
				$\vec{x_5}(1{:}T^c)= V_{DS}$	Drain-Source Voltage
				$\vec{x_6}(1{:}T^c)= I_G$	Gate Current
	$o_3 = f_{switch}$	Switching Frequency		$\vec{x_7}(1{:}T^c)= I_D$	Drain Current
				$\vec{x_8}(1{:}T^c) = V_{load}$	Load Voltage
				$\vec{x_9}(1{:}T^c) = I_{load}$	Load Current

- variations of the external temperature (T_{ext}), which are due to the seasonal oscillations of the ambient temperature and modifications the heat provided by the motor; the variability of T_{ext} is modeled using a normal distribution with mean equal to 350.5K and standard deviation of 10K;

- measurements errors, which are modeled using zero-mean normal distribution. The error's standard deviation has been taken from commercial sensors datasheets (Ulrich 2019) (Avenas and Dupont 2012);

- errors of the control system used to perform the AATs, which depend on the delay of the thermal sensor in following the very fast variations of $Tcase$. The delay is represented by a normal distribution with zero mean and standard deviation of 5K.

3.2. Degradation model

We compute the switch degradation, D, using the Miner's rule (Held, et al. 1999) (Kovačević, Drofenik and Kolar 2010):

$$D = \sum_{all\ the\ stress\ levels} \frac{N_k}{N_{fk}} \qquad (1)$$

where, N_k is the number of thermal cycles performed by the MOSFET at the $k-th$ stress level, and N_{fk} is the number of cycles which would lead to failure a new MOSFET at that stress level. Although, in practice, the accurate modeling of an AAT would require to use $N_k = 1$ since each thermal cycle is degrading the MOSFET and, therefore, the next cycle is expected to be different, in practice, the degradation of a single thermal cycle is considered small and N_k is set equal to 50 for reducing the computational cost. According to this model the component is assumed to fail when the degradation D reaches 1.

The number of cycles to failure, N_{fk}, which depends from the average ($\overline{T_j}$) and swing (ΔT_j) junction temperatures, is (Held, et al. 1999):

$$N_{fi} = A \Delta T_j^{\alpha} e^{\left(\frac{Q}{R \times \overline{T_j}}\right)} \qquad (2)$$

where, $A = 640$ and $\alpha = -5$ are empirical constants, $Q = 7.8 * 10^{14}$ j/mol and R is the gas constant. Eq. (2), which is based on the Arrhenius law, has been adopted since experimental tests suggest that switches degradation is mainly caused by thermally activated creeping processes. The following sources of uncertainty have been injected in the simulations to properly represent the stochastic nature of the degradation phenomenon (Table 2):

- Uncertainty on the damage produced by the thermal cycle; each term of the sum in Eq. (1) is multiplied by (1+N) where N is a gaussian noise with zero mean and standard deviation equal to the 2%;

- Uncertainty on the parameters of the degradation model M_{deg}; the gaussian noises with zero mean and standard deviations reported in Table 2 are added to their values.

Table 2: Sources of uncertainty on the degradation process and their representation

Uncertainty source	Signals	Quantification	Frequency of injection
Degradation	Degradation increment	× N(0, 2%)	Every cycle
Model Parameters	Q→ $Q_0 = 7.8 * 10^4$	× N(0, 0.5%)	Every device
	A→ $A_0 = 640$	+ N (0, 5)	
	α → $\alpha_0 = -5$	+ N (0, 0.1)	

3.3. Resistance model

According to (Dusmez, Duran and Akin 2016) the main effect of the degradation of the MOSFET on its properties is the increase of Rds. In this work, we assume that the function relating D and Rds is linear. Therefore Rds of a device with degradation level D can be computed as:

$$Rds = Rds_0 + \alpha * D \qquad (3)$$

where the initial value of the resistance Rds_0 is directly provided by the producer, parameter α is set in such a way that when $D = 1$ the component fails, i.e. the junction temperature T_j exceeds a threshold value, $T_{j,limit}$, typically provided by the producer. Since the relation between Rds and T_j depends from the operational conditions ($\vec{o}$), also the parameter α depends from the operational conditions, $\alpha = \alpha(\vec{o})$. The operative procedure for the estimation of α in the operational conditions $\vec{o}$ is based on a trial-and-error approach and uses the model $M_{H-bridge}$ for the identification of Rds_{max}, i.e. the value of Rds corresponding to a junction temperature equal to $T_{j,limit}$ (448K in our application).

4. Prognostic Model

The data simulated with the model described in Section 3 are used to train a data-driven prognostic model with the objective of predicting the RUL of the MOSFETs.

Specifically, an ensemble of ANNs has been developed (Figure 3). The choice is motivated by the fact that the combination of the outcomes of an ensemble of models has been shown to be more accurate and robust to uncertainties than the use of a single "best" model (Kourentzes, Barrow and Crone 2014). In the present work, the individual models of the ensemble have been trained using different sets of data. In particular, the original dataset has been randomly split in L subsets without resampling and a different combination of subsets is used to train each one of the L models of the ensemble. With reference to the aggregation of the models outcomes, the median has been chosen since it is more robust to possible outliers among the ensemble outcomes than other statistical indicators such as the sample mean (Kourentzes, Barrow and Crone 2014).

As individual model of the ensemble, an ANN with one hidden layer has been chosen due to its possibility of modelling nonlinear input-output relationships and the limited amount of computational effort needed for its training. To properly capture the dynamic of the degradation process, which does not allow to accurately predict the RUL using only signal values measured at a given time, the set of input to the ANN is formed by the signal values in a time window of 3 timesteps.

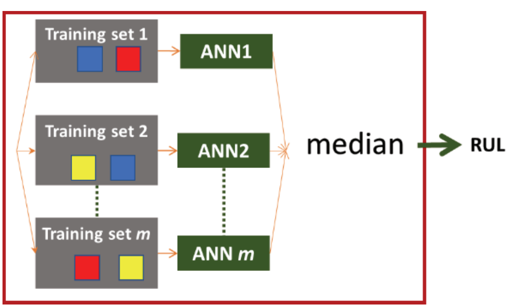

Figure 3: Developed prognostic model.

5. Application

5.1. Dataset description

A total of 160 run to failure trajectories have been simulated using the model of Section 3. They are split in a training set of 105 trajectories, a validation set of 35 trajectories and a test set of 20 trajectories. Training and validation sets are used to develop the ensemble of ANNs and tune their hyperparameters. The test set is used for the final evaluation of the model performance.

We consider as unit of measurement of the RUL the number of thermal cycles, i.e. the RUL indicates the number of remaining thermal cycles before failure.

5.2. Feature extraction

The physical quantities that we consider as input to the ANNs are the external temperature T_{ext}, due to its influence on the degradation process, and all the simulated signals reported in Table 1, except the junction temperature T_j, which is typically difficult to measure in field applications. The information about the evolution of the signals during a thermal cycle is compressed using the following lumped statistical features: mean, standard deviation, minimum and maximum values. To capture the dynamical behavior of the system, we provided in input to the ANN the values of the extracted features in 3 cycles taken every 50 cycles: $y(i)$, $y(i-50)$, $y(i-100)$. Therefore, the total number of input features to the ANNs is 108 (9 physical quantities $\times 4$ features per physical quantity $\times$ 3 cycles for feature).

5.3. Performance metrics

The performance metrics used to evaluate the prognostic performances are: Cumulative Relative Accuracy (CRA), $\alpha - \lambda$ and Mean Square Error (MSE):

$$CRA = 1 - \sum \frac{\widehat{RUL(\iota)} - RUL(i)}{RUL(i)} \quad (4)$$

$$(\alpha - \lambda)_i = \begin{Bmatrix} 0 \; if \left|\widehat{RUL(\iota)} - RUL(i)\right| > RUL(i) \times \alpha \\ 1 \; if \left|\widehat{RUL(\iota)} - RUL(i)\right| < RUL(i) \times \alpha \end{Bmatrix}$$

$$\rightarrow \alpha - \lambda = E[(\alpha - \lambda)_i] \quad (5)$$

$$MSE = \frac{\sum \left(\widehat{RUL(\iota)} - RUL(i)\right)^2}{N} \quad (6)$$

where $\widehat{RUL(\iota)}$ is the estimated RUL at the *i-th* thermal cycle, α is the percentage of acceptable error and N is the total number of thermal cycles. The MSE is to be minimized and is used both for performance evaluation and for training the ANNs. CRA and $\alpha - \lambda$, instead, are contained in [0,1], are to be maximized and are used for performance evaluation only.

5.4. ANN parameter setting

The values of the ANNs' hyperparameters (number of neurons in the hidden layer and the batch size) are optimized using a grid search procedure. The best performance in terms of MSE has been obtained using 20 neurons and a batch size of 10 patterns. The number of individual models of the ensemble has been set equal to 4.

5.5. Results

Figure 4 shows the predictions of the RUL of a run-to-failure trajectory provided by the developed ensemble model and by its individual ANNs. Notice that the ensemble outcome, i.e. the median of the individual models outcomes, is not affected by the non-satisfactory prediction of one of the four models. This confirms the robustness of the ensemble towards single model possible large errors, which can be caused, for example, by their training set composition.

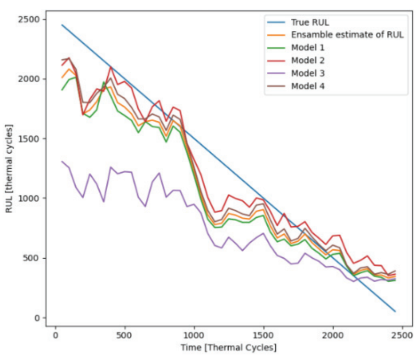

Figure 4: Prediction of the RUL of one test trajectory by the proposed method and its individual models.

Table 3: Performance of the 4 individual ANNs, the proposed ensemble approach and the case in which the input features refer only to the present thermal cycle.

	Average	Ensemble	No dynamic
CRA	**20,52 %**	**20,67 %**	9.42%
$\alpha - \lambda$	**28,53 %**	**29, 32 %**	23.21%
$RMSE$ [$th\ cycle$	**803**	**760**	926

Figure 5 shows the effect of using in input to the ANNs the time window of the signals. As expected the accuracy of the RUL predictions when accounting for previous thermal cycles improves, especially at the beginning and at the end of the life. The overall test performances are reported in Table 3 considering the metrices of CRA, $\alpha - \lambda$ and MSE. The table reports the comparison between the average performances of the four individual ANNs, of the proposed ensemble and of an ensemble whose ANNs are fed by features referring to only the present thermal cycle. The results confirm that the developed ensemble slightly overperforms a single ANN model and the significative improvement of the performance obtained by providing in input to the model a sliding window of signal values.

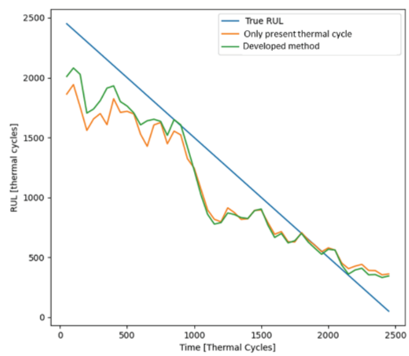

Figure 5: RUL provided by the proposed model and by an ensemble of ANNs which receives in input only the features extracted from the current thermal cycle.

6. Conclusions

This work has considered the problem of fault prognostics in EV inverters, focusing on its most critical components, i.e. switches. Specifically we have considered MOSFETs of a H-bridge inverter. The main challenge addressed is the lack of real data to develop data-driven prognostic models. To properly address the challenge, we have firstly developed a physics-based model for the simulation of AATs in various operational and external conditions. Then, a data-driven fault prognostic model based on an ensemble of ANNs, which receive in input sliding windows of the measured signals, has been developed.

The main contributions of the work are the integration of a MOSFET Simulink model with a physics-based degradation model has allowed the simulation of run-to-failure trajectories; and the achievement of a significative improvement of the RUL prediction accuracy by using an ensemble of ANNs which receive in input sliding windows of the measured signals.

Future developments will aim at validating the simulator with laboratory data and at exploring more advanced ANNs architectures such as LSTM to account for the dynamical behaviour of the system.

Acknowledgement

iRel40 is a European co-funded innovation project that has been granted by the ECSEL Joint Undertaking (JU) under grant agreement No 876659. The funding of the project comes from the Horizon 2020 research programme and participating countries. National funding is provided by Germany, including the Free States of Saxony and Thuringia, Austria, Belgium, Finland, France, Italy, the Netherlands, Slovakia, Spain, Sweden, and Turkey.

Disclaimer:

"The document reflects only the author's view and the JU is not responsible for any use that may be made of the information it contains."

References

Avenas, Y., and L. Dupont. 2012. "Evaluation of IGBT thermo-sensitive electrical parameters under different dissipation conditions - Comparison with infrared measurements.". 52(11)

Banerjee, Ahin, Chandrasekhar Putcha, and Sanjay K. Gupta. 2021. Particle Filter Based Prognostic Approach for Automotive Motor.

Ciappa, Mauro. 2002. "Selected failure mechanisms of modern power modules." Microelectronics Reliability 42 (4-5).

Dusmez, Serkan, Hamit Duran, and Bilal Akin. 2016. Remaining Useful Lifetime Estimation for Thermally Stressed Power MOSFETs Based on on-State Resistance Variation. Vol. 52.

Heimes, Felix O. 2008. Recurrent neural networks for remaining useful life estimation.

Held, M., P. Jacob, G. Nicoletti, P. Scacco, and M. H. Poech. 1999. "Fast power cycling test for insulated gate bipolar transistor modules in traction application." International Journal of Electronics 86 (10).

Hochreiter, Sepp, and Jürgen Schmidhuber. 1997. "Long Short-Term Memory." Neural Computation 9 (8).

Ji, Bing, Volker Pickert, Wenping Cao, and Bashar Zahawi. 2013. In situ diagnostics and prognostics of wire bonding faults in IGBT modules for electric vehicle drives. Vol. 28.

Khan, Alif Md Asif, Siam Hasan Khan, and Ahmed Mortuza Saleque. 2018. "H-Bridge Driven Propulsion System for a Light Weight Electric Vehicle using DC Link Voltage Controller."

Kourentzes, Nikolaos, Devon K. Barrow, and Sven F. Crone. 2014. "Neural network ensemble operators for time series forecasting." Vol. 41. no. 9.

Kovačević, I. F., U. Drofenik, and J. W. Kolar. 2010. "New physical model for lifetime estimation of power modules." 2010 International Power Electronics Conference - ECCE Asia -, IPEC 2010.

Ni, Ze, Xiaofeng Lyu, Om Prakash Yadav, Brij N. Singh, Sheng Zheng, and Dong Cao. 2020. "Overview of real-time lifetime prediction and extension for SiC power converters." 35(8).

Niu, Gang. 2017. Design Approach for Systems Health Management.

Peel, Leto. 2008. Data driven prognostics using a kalman filter ensemble of neural network models.

Sepahvand, Hossein, Jingsheng Liao, Mehdi Ferdowsi, and Keith A. Corzine. 2013. "Capacitor voltage regulation in single-DC-source cascaded H-bridge multilevel converters using phase-shift modulation.". 60(9).

Si, Xiao Sheng, Wenbin Wang, Chang Hua Hu, and Dong Hua Zhou. 2011. Remaining useful life estimation - A review on the statistical data driven approaches. Vol. 213.

Silva, R. E., R. Gouriveau, S. Jemeï, D. Hissel, L. Boulon, K. Agbossou, and N. Yousfi Steiner. 2014. Proton exchange membrane fuel cell degradation prediction based on Adaptive Neuro-Fuzzy Inference Systems. Vol. 39.

Singh, Vineeta, and G. L. Pahuja. 2018. Failure modes and effects analysis using fuzzy logic for electric vehicle inverter.

Sutharssan, Thamo, Stoyan Stoyanov, Chris Bailey, and Chunyan Yin. 2015. Prognostic and health management for engineering systems: a review of the data-driven approach and algorithms. Vol. 2015.

Ulrich, Burkhard. 2019. "Open-source wideband (DC to MHz range) isolated current sensor." 5.

Wang, Bing, Guangdong Tian, Yanping Liang, and Tiangang Qiang. 2014. Reliability modeling and evaluation of electric vehicle motor by using fault tree and extended stochastic petri nets. 2014.

Wang, Huai, Marco Liserre, and Frede Blaabjerg. 2013. Toward reliable power electronics: Challenges, design tools, and opportunities. Vol. 7.

Zio, Enrico, and Francesco Di Maio. 2010. A data-driven fuzzy approach for predicting the remaining useful life in dynamic failure scenarios of a nuclear system. Vol. 95.